Appendix D

Short operators by Generalized Fourier Transformation

Jan Thorbecke

D.1 Introduction

From wave theory analysis it is known that many wave field operators have an exact expression in the wavenumber-frequency domain for laterally homogeneous isotropic media. For example, the extrapolation and elastic decomposition operators have both a simple analytical expression in the wavenumber-frequency domain. The spatial equivalents of these operators are often complex expressions (if they exist at all) and are not decaying in amplitude for larger offsets. From a computational point of view long spatial operators are not desired because multiplication in the wavenumber-frequency domain is replaced by a convolution in the space-frequency domain. In this Appendix we will consider a method for calculating an optimized short spatial operator by transforming, in a non standard way, the expression of the operator in the wavenumber-frequency domain back to the space-frequency domain. This method is explained with the decomposition operators at the receiver side as a leading example.

D.2 Analytical space-frequency operators

We will first derive the analytical expressions of the decomposition operators in the space-frequency domain to show that these operators are too long to be used in practice and that band-limitation of these operators is very important in the decomposition process. The decomposition operators at the receiver side (particle velocity detectors) are given by (Wapenaar, 1989):

$$\left[\boldsymbol{D}^{-}\right]^{-1} = \boldsymbol{M}^{-} = \begin{pmatrix} \boldsymbol{M}_{11}^{-} & \boldsymbol{M}_{12}^{-} \\ \boldsymbol{M}_{21}^{-} & \boldsymbol{M}_{22}^{-} \end{pmatrix} = \frac{\mu}{2\omega} \begin{bmatrix} 2k_x & -\dfrac{\left(k_s^2 - 2k_x^2\right)}{k_{z,p}} \\ \dfrac{\left(k_s^2 - 2k_x^2\right)}{k_{z,s}} & 2k_x \end{bmatrix} \tag{D.1}$$

with

$$\begin{aligned} k_p &= \frac{\omega}{c_p} \\ k_{z,p} &= \sqrt{k_p^2 - k_x^2} \\ k_s &= \frac{\omega}{c_s} \\ k_{z,s} &= \sqrt{k_s^2 - k_x^2} \end{aligned} \tag{D.2}$$

The analytical wavenumber spectra for M_{ij}^{-} are, for one frequency, shown in Figure D.1.

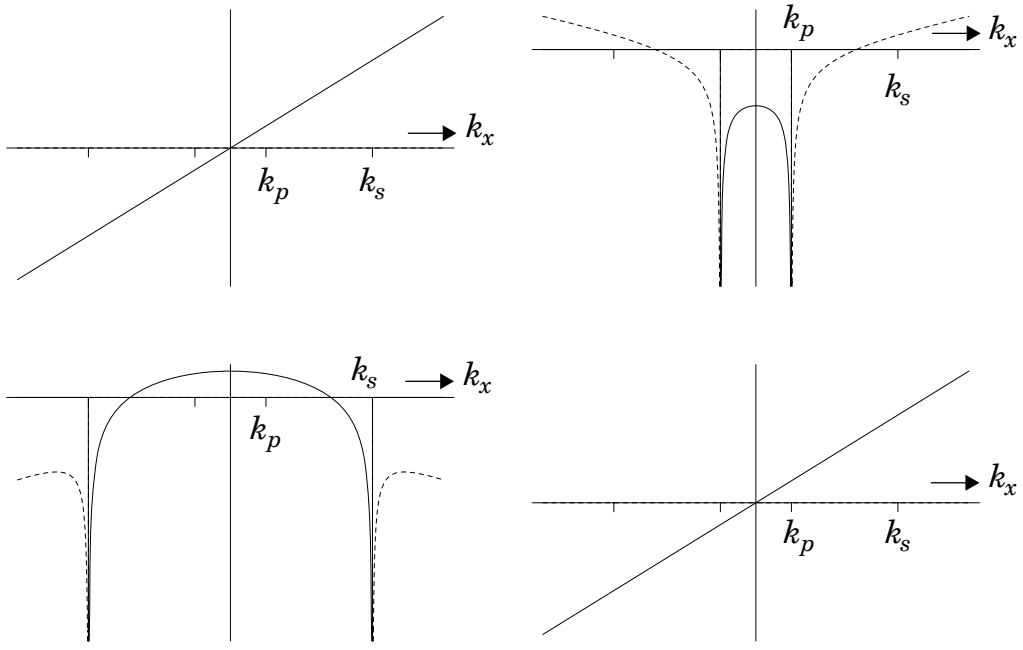

Fig. D.1 *Components of the* $\boldsymbol{M}^{-}$ *decomposition operator with* $C_s = 500$ m/s *and* $C_p = 2000$ m/s

It is not trivial to calculate these decomposition operators analytically in the space-frequency domain by analytically solving the integral of the inverse Fourier transform over *all* wavenumbers. But it is possible to calculate a bandlimited solution for the M_{12}^{-} and M_{21}^{-} operators. Further the M_{11}^{-} and M_{22}^{-} operators can be recognized as a differentiation with respect to the

spatial coordinate. These two observations are used to derive 'analytical' expressions for the decomposition operators in the space-frequency domain.

Before we start with the derivation of the bandlimited M_{12}^{-} and M_{21}^{-} decomposition operators we will first discuss some properties of the Bessel functions which are needed in the derivation. According to Abramowitz and Stegun (formula 9.1.21) the nth order Bessel function of the first kind is defined as (for integer n)

$$\begin{aligned} \mathrm{J}_n(z) &= \frac{1}{\pi}\int_0^{\pi} \cos(z\sin(\phi) - n\phi)d\phi \\ &= \frac{j^{-n}}{\pi}\int_0^{\pi} \exp(jz\cos(\phi))\cos(n\phi)d\phi \end{aligned} \tag{D.3}$$

by replacing $\cos\phi = \sin(\phi + \frac{\pi}{2})$ and substituting $\phi = \varphi + \frac{\pi}{2}$ in equation (D.3) we arrive at

$$\mathrm{J}_n(z) = \frac{j^{-n}}{\pi}\int_{-\frac{\pi}{2}}^{\frac{\pi}{2}} \exp(-jz\sin(\varphi))\cos(n(\varphi + \frac{\pi}{2})d\varphi\,. \tag{D.4}$$

For the zero order Bessel function of the first kind (n = 0) equation (D.4) can be written as

$$\mathrm{J}_0(z) = \frac{1}{\pi}\int_{-\frac{\pi}{2}}^{\frac{\pi}{2}} \exp(jz\sin(\varphi))d\varphi\,, \tag{D.5}$$

where the minus sign in the exponent is be omitted because the zero order Bessel function is an even function.

The first order Bessel function of the first kind can be written as

$$\mathrm{J}_1(z) = \frac{1}{\pi j}\int_{-\frac{\pi}{2}}^{\frac{\pi}{2}} \exp(-jz\sin(\varphi))\sin(\varphi)d\varphi\,. \tag{D.6}$$

And finally the last function we need, the second order Bessel function of the first kind is defined by the expression

$$\mathrm{J}_2(z) = \frac{-1}{\pi}\int_{-\frac{\pi}{2}}^{\frac{\pi}{2}} \exp(-jz\sin(\varphi))\cos(2\varphi+\pi)d\varphi$$

$$= \frac{1}{\pi}\int_{-\frac{\pi}{2}}^{\frac{\pi}{2}} \exp(-jz\sin(\varphi))d\varphi - \frac{2}{\pi}\int_{-\frac{\pi}{2}}^{\frac{\pi}{2}} \exp(-jz\sin(\varphi))\sin^2(\varphi)d\varphi\,. \tag{D.7}$$

The second term of the last expression (the integral with the $\sin^2$ in it) can be written as

$$\frac{2}{\pi}\int_{-\frac{\pi}{2}}^{\frac{\pi}{2}} \exp(-jz\sin(\varphi))\sin^2(\varphi)d\varphi = \mathrm{J}_0(z) - \mathrm{J}_2(z). \tag{D.8}$$

Now we can return to two of our four decomposition operators given by M_{12}^- and M_{21}^- in equation (D.1). The bandlimited inverse Fourier transform of these operators is defined as

$$M_{12}^-(x,\omega) = \frac{-\mu}{2\pi\omega}\int_{-k_p}^{k_p} \frac{\left(k_s^2 - 2k_x^2\right)}{2k_{z,p}} \exp(-jk_x x)dk_x\,, \tag{D.9}$$

$$M_{21}^-(x,\omega) = \frac{\mu}{2\pi\omega}\int_{-k_s}^{k_s} \frac{\left(k_s^2 - 2k_x^2\right)}{2k_{z,s}} \exp(-jk_x x)dk_x\,. \tag{D.10}$$

The integration intervals are chosen at $|k_x| < k_p$ for the M_{12}^- operator and $|k_x| < k_s$ for the M_{21}^- operator. By making this restriction for the M_{12}^- operator we are neglecting all evanescent waves in the resulting P wave recordings and are excluding a part of the S-waves (for the S-wave it means that the range $k_p < |k_x| < k_s$ is not properly treated). This restriction is for the P-waves a valid restriction because the receivers don't measure the evanescent waves and in the P-wave field no S-energy should be present. We will first derive the bandlimited inverse transform of equation (D.9).

By making the variable substitutions

$$\begin{aligned} k_x &= k_p\sin(\alpha) \\ k_{z,p} &= k_p\cos(\alpha) \\ dk_x &= k_p\cos(\alpha)d\alpha \end{aligned} \tag{D.11}$$

the integral of equation (D.9) can be written in a convenient way with respect to the expressions, derived above, for the Bessel functions. Using equations(D.11), equation (D.9) changes into

$$M_{12}^{-}(x,\omega) = -\frac{\mu}{4\omega\pi}\int_{-\frac{\pi}{2}}^{\frac{\pi}{2}}(k_s^2 - 2k_p^2\sin^2(\alpha))\exp(-jk_p x\sin(\alpha))d\alpha \tag{D.12}$$

or

$$M_{12}^{-}(x,\omega) = -\frac{\mu}{4\omega}\left\{\frac{k_s^2}{\pi}\int_{-\frac{\pi}{2}}^{\frac{\pi}{2}}\exp(-jk_p x\sin(\alpha))d\alpha - \frac{k_p^2}{\pi}\int_{-\frac{\pi}{2}}^{\frac{\pi}{2}}2\sin^2(\alpha))\exp(-jk_p x\sin(\alpha))d\alpha\right\} \tag{D.13}$$

Making use of the expressions for the Bessel functions, given in equation (D.5) and equation (D.8), we finally arrive at

$$M_{12}^{-}(x,\omega) = -\frac{\mu}{4\omega}\left\{(k_s^2 - k_p^2)\,\mathrm{J}_0\left(k_p x\right) + k_p^2\,\mathrm{J}_2\left(k_p x\right)\right\} \tag{D.14}$$

for $|k_x| < k_p$.

Analogous to the previous derivation the M_{21}^{-} operator can be written as

$$\begin{aligned} M_{21}^{-}(x,\omega) &= \frac{\mu}{4\pi\omega}\int_{-\frac{\pi}{2}}^{\frac{\pi}{2}}k_s^2\cos(2\alpha)\exp(-jk_s x\sin(\alpha))d\alpha \\ &= \frac{\mu}{4\omega}k_s^2\,\mathrm{J}_2\left(k_s x\right) \end{aligned} \quad , \tag{D.15}$$

for $|k_x| < k_s$.

The bandlimited 'analytical' M_{12}^{-} and M_{21}^{-} operators are shown, for a 500 meter long operator, in Figure D.2. The operators are slowly decaying for increasing offsets. So for an accurate computation a long operator must be used as convolution operator in the space-frequency domain. Note that the M_{21}^{-} operator oscillates more rapidly than the M_{12}^{-} operator due to the fact that the wave length for S-waves is four times as short as the wave length for P-waves.

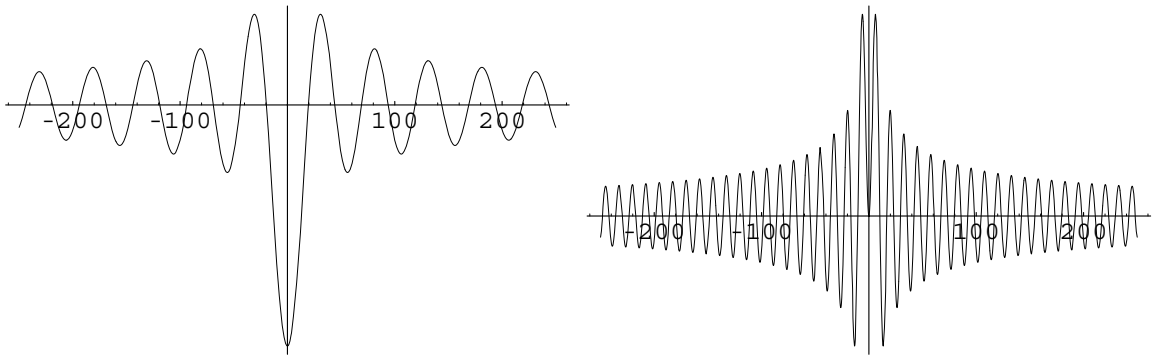

(a)M^-_{12}operator *(b)M^-_{21}operator*

Fig. D.2 *Bandlimited 'analytical' M^-_{12} (a) and M^-_{21} (b) operator.*

The two other decomposition operators $M^-_{11} = M^-_{22}$ are not transformed back in the same analytical bandlimited way. From Fourier analysis it is known that differentiation in the space-frequency domain is equivalent with multiplication by $-ik_x$ in the wavenumber-frequency domain. The $M^-_{11} = M^-_{22}$ operators are a scaled differentiation with respect to the spatial x-coordinate. Numerical differentiation is a well-known subject which has many good solutions, so we only have to look for a short and suitable numerical differentiation operator in order to arrive at a good approximation of the spatial decomposition operator. Abramowitz and Stegun give in equation 25.3.6 and in table 25.2 a five point differentiation operator which we could use in our calculations (see Table D-1 and equation (D.16)).

$$\left.\frac{d\,\mathrm{f}(x)}{dx}\right|_{x=x_j} \approx \frac{1}{m!h}\sum_{i=0}^{m} A_i\,\mathrm{f}(x_i)\,,\; m = 4\,. \tag{D.16}$$

Table D-1 *Five point differentiation operator (m=4) for equally spaced abscissas.*

j	A_0	A_1	A_2	A_3	A_4
0	-50	96	-72	32	-6
1	-6	-20	36	-12	2
2	2	-16	0	16	-2
3	-2	12	-36	20	6
4	6	-32	72	-96	50

If we actually do the calculation for the P-wave we would see some S-wave energy left in the P-wave panel. This residue could be expected because we have calculated the M^-_{12} operator up to k_p, but the M^-_{11} operator is calculated over a broader band which also includes the higher

angles of incidence for the S-wave. So for higher angles of incidence the S-wave is not completely removed in the summation of the V_x and the V_z records. (The V_x and the V_z records are convolved with their decomposition operator which have a different wavenumber-frequency band; these results are added together to construct the P-wave panel.) If there is an expression for a suited bandlimited differentiation operator we should use this one and the problem would be solved. Another, less serious, problem are the lengthy M_{12}^- and M_{21}^- operators. The length of the operators makes the computation time too long to be useful in practice. Truncating of these long operators will give raise to unwanted artefacts in the decomposed panels. From the foregoing results we have learned that bandlimitation and truncation are important issues in deriving space-frequency operators from wavenumber-frequency operators. In the next section we will use this observation to develop a more successful and practical approach.

D.3 Space-frequency operators from weighted least squares

The most simple way to obtain numerically the space-frequency decomposition operators is to transform the discrete decomposition operators in the wavenumber-frequency domain numerically back to the space-frequency domain. But this simple solution is not very efficient because the spatial convolution operator obtained in this way is still very long. What we are looking for is a short decomposition operator with a wavenumber-frequency spectrum which is, over a desired wavenumber band, equal or close to the exact formulation in the k_x-ω domain. This problem can be written as an integral equation which is given by

$$\tilde{\mathrm{Y}}(k_x) = \int_{x_1}^{x_2} \exp(jk_x x)\,\mathrm{Y}(x)dx \quad \text{for } k_1 \le k_x \le k_2\,. \tag{D.17}$$

In this integral equation we are integrating over a limited spatial domain (short operator) and the wavenumber-frequency spectrum of the decomposition operator is bandlimited. The discrete counterpart of this integral equation is

$$\tilde{\mathrm{Y}}(n\Delta k_x) = \Delta x \sum_{\mathrm{M}_1}^{\mathrm{M}_2} \exp(jn\Delta k_x m\Delta x)\,\mathrm{Y}(m\Delta x) \quad \text{for } N_1 \le n \le N_2\,. \tag{D.18}$$

Written more explicitly in matrix notation

$$\begin{pmatrix} \tilde{\mathrm{Y}}(N_1\Delta k_x) \\ \vdots \\ \vdots \\ \tilde{\mathrm{Y}}(0) \\ \vdots \\ \vdots \\ \tilde{\mathrm{Y}}(N_2\Delta k_x) \end{pmatrix} = \begin{pmatrix} \exp(jN_1\Delta k_x M_1\Delta x) & \cdots & 1 & \cdots & \exp(jN_1\Delta k_x M_2\Delta x) \\ \vdots & & \vdots & & \vdots \\ \vdots & & \vdots & & \vdots \\ 1 & \cdots & 1 & \cdots & 1 \\ \vdots & & \vdots & & \vdots \\ \vdots & & \vdots & & \vdots \\ \exp(jN_2\Delta k_x M_1\Delta x) & \cdots & 1 & \cdots & \exp(jN_2\Delta k_x M_2\Delta x) \end{pmatrix} \begin{pmatrix} \Delta x\,\mathrm{Y}(M_1\Delta x) \\ \vdots \\ \Delta x\,\mathrm{Y}(0) \\ \vdots \\ \Delta x\,\mathrm{Y}(M_2\Delta x) \end{pmatrix}$$

or

$$\vec{\tilde{\mathrm{Y}}} = \boldsymbol{F}\,\vec{\mathrm{Y}} \tag{D.19}$$

with m = M_1..... M_2 the length of the desired short operator and n = N_1..... N_2 the length of the Fourier transformation and

$$\Delta k_x = \frac{2\pi}{(N_1 + N_2 + 1)\Delta x}. \tag{D.20}$$

The number of samples in the wavenumber-frequency domain must be chosen in such a way that the short spatial operator is zero outside its working lenght. This means that the number of samples in the wavenumber-frequency domain must be greater or equal to the number of receivers in the spatial domain.

Because matrix equation (D.19) has more equations than unknowns, it is usually impossible to find a unique solution which satisfies all the equations. To solve this problem we have to look for a solution which approximately satisfies all the equations in a least squares manner. We define therefore an error function ε which is given by

$$\varepsilon = \vec{\mathrm{E}}^h\,\boldsymbol{\Lambda}\,\vec{\mathrm{E}} \tag{D.21}$$

with

$$\vec{\mathrm{E}} = \boldsymbol{F}\,\vec{\mathrm{Y}} - \vec{\tilde{\mathrm{Y}}} \tag{D.22}$$

and try to minimize this error (superscript *h* denotes complex-conjugate transpose). Because we want to solve the matrix system for only those wavenumber values which are relevant for our problem, we have introduced a weighting function $\boldsymbol{\Lambda}$ (Herrmann, 1992). By introducing this weighting function we have a good control over the desired *function* of the space-frequency operators. The least squares solution of equation (D.21) is given by the following equation

$$\frac{\partial\varepsilon}{\partial(Y^h)_i} = 0 \qquad \forall(Y^h)_i \tag{D.23}$$

with

$$\varepsilon = \left(\vec{\mathrm{Y}}^{h} \boldsymbol{F}^{h} - \vec{\tilde{\mathrm{Y}}}^{h} \right) \boldsymbol{\Lambda} \left(\boldsymbol{F} \vec{\mathrm{Y}} - \vec{\tilde{\mathrm{Y}}} \right) \tag{D.24}$$

The solution of equation (D.23) is given by (slightly modified after Claerbout, 1985)

$$\boldsymbol{F}^{h} \boldsymbol{\Lambda} \left(\boldsymbol{F} \vec{\mathrm{Y}} - \vec{\tilde{\mathrm{Y}}} \right) = \vec{0} \,, \tag{D.25}$$

or

$$\vec{\mathrm{Y}} = \left[\boldsymbol{F}^{h} \boldsymbol{\Lambda} \boldsymbol{F} \right]^{-1} \boldsymbol{F}^{h} \boldsymbol{\Lambda} \vec{\tilde{\mathrm{Y}}} \,. \tag{D.26}$$

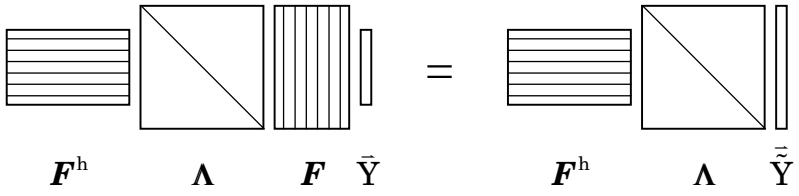

Fig. D.3 *Weighted least squares solution of a matrix equation.*

In Figure D.3 the weighted least squares solution is given in a matrix scheme. The components of the Fourier transformation and the inverse Fourier transformation matrices are given by

$$F_{nm} = \exp\left(jn\Delta k_x m\Delta x \right), \tag{D.27}$$

$$F^{h}_{mn} = \exp\left(-jn\Delta k_x m\Delta x \right). \tag{D.28}$$

The weight function, which is a diagonal matrix, is given by

$$\Lambda_{nm} = w\left(n\Delta k_x \right) \delta_{nm} \,. \tag{D.29}$$

The total matrix $\boldsymbol{F}^{h} \boldsymbol{\Lambda} \boldsymbol{F}$ which stands before the unknown is a MxM matrix and has a Toeplitz structure:

$$\left(\boldsymbol{F}^{h} \boldsymbol{\Lambda} \boldsymbol{F} \right)_{ml} = \sum_{n} w\left(n\Delta k_x \right) \exp\left(jn\Delta k_x (m-l)\Delta x \right). \tag{D.30}$$

This matrix can be inverted relatively fast by using a Levinson scheme (see for example Claerbout (1985) page 53-57).

If we take in equation (D.26) the weight matrix identical to the unit matrix $\boldsymbol{I}$ then the right hand side of equation (D.26) is an inverse Fourier transform (N-points) which is reduced (by truncating) to M points in the spatial domain. In this specific case no optimization is carried out. How effective the optimization can be is illustrated below with the decomposition operators shown in the previous section.

The optimization procedure is only effective if we can define a wavenumber spectrum in which the decomposition operator must be accurate. Figure D.4 shows different domains in the wavenumber-frequency domain. There are three bandlimitations;

- limited temporal frequency range,
- maximum angle of propagation,
- Nyquist wavenumber $\pm\pi/\Delta x$

These three bandlimitations determine together the domain of interest for the different decomposition operators. In seismic experiments we don't measure the evanescent waves, so we can neglect all the information which goes beyond the maximum angle of propagation α_{max}(the white area in Figure D.4). For the P-waves we can also neglect the light shaded area. Recordings are discrete so there is a Nyquist wavenumber which limits the maximum operator angle for a given frequency. This angle is declining for higher frequencies because of the aliasing of the wavenumber-frequency spectrum.

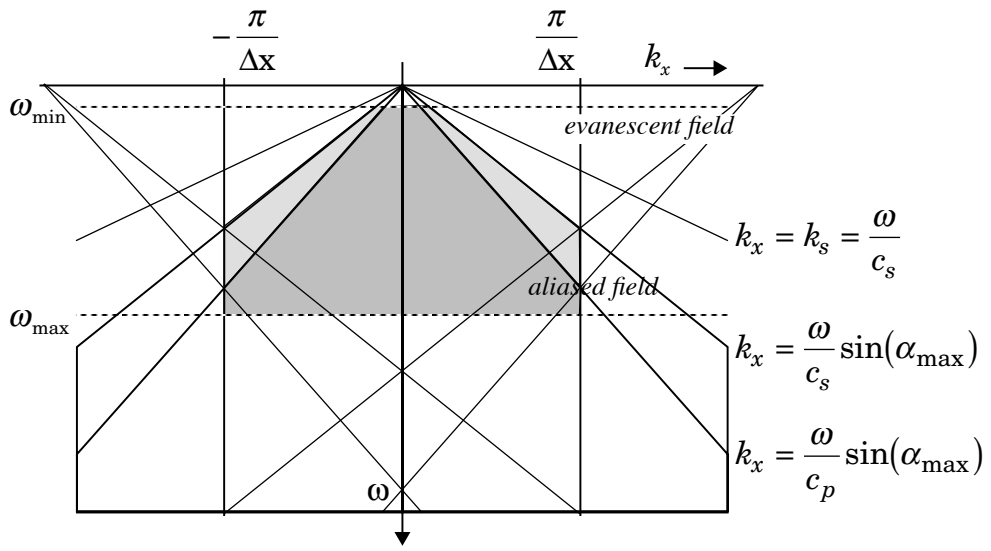

Fig. D.4 *Wavenumber-frequency domain subdivided in different domains of interest.*

According to these considerations a strategy is developed in which the decomposition operators are only calculated in their specific band of interest. In Figure D.5 these bandlimited operators are displayed, assuming that the maximum angle og propagation = 90° and that $k_s < \pi/\Delta x$. Comparing these operators with Figure D.1 we see that the band of interest is specific for each operator; for example the M_{11}^- operator must be accurate for $|k_x| < k_p$., for $k_p < |k_x| < k_s$ it must be zero, and for $|k_x| > k_s$ it can, in theory, be anything because in this area there is no seismic energy. The weight function in the least squares solution must be designed in such a way that it satisfies these specific bands for each operator.

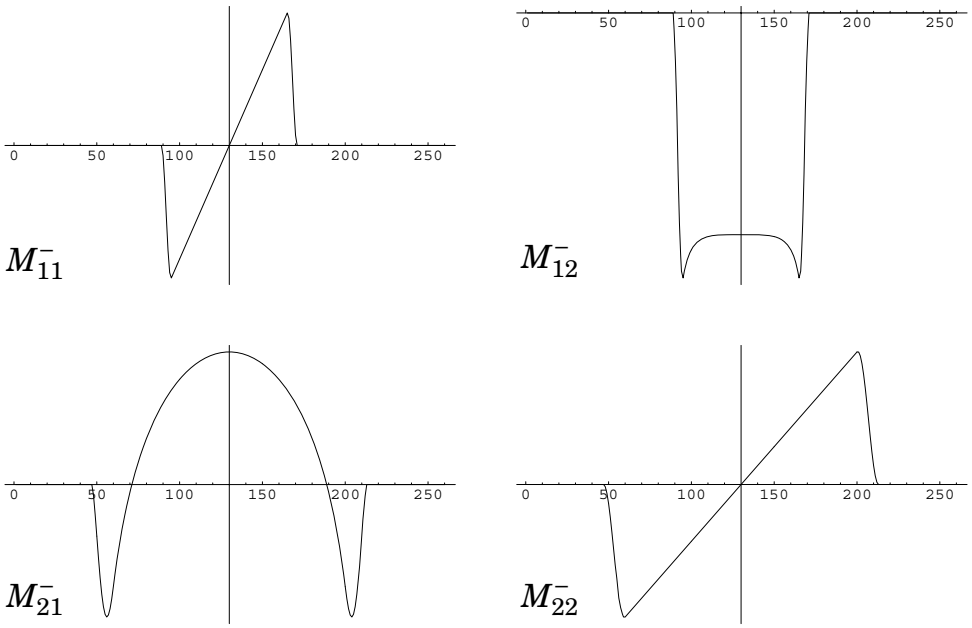

Fig. D.5 *Bandlimited decomposition operators for one frequency.*

In Figure D.6 the spatial decomposition operators are shown together with their wavenumber spectrum where a unit weight function is used (no optimization). Thus in Figure D.6 the space--frequency operators are obtained by truncating the inverse Fourier transform of the operators in Figure D.5 to 29 points. To make a comparison in the wavenumber domain these spatial operators are padded with zero's to 260 points and transformed to the wavenumber domain(right pictures).

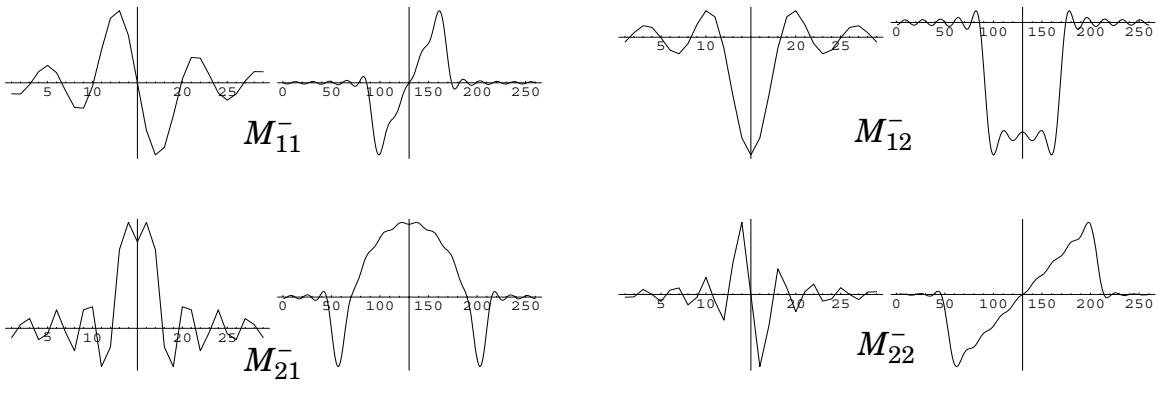

Fig. D.6 *Spatial decomposition operators calculated with unit weight function (meaning truncation). Left is the spatial operator, right the real part of the wavenumber spectrum of this operator. The numbers on the horizontal axis indicate the number of discrete points.*

In Figure D.6 the optimized spatial decomposition operators are shown. The band specific weight function we used is shown in Figure D.8. The P-wave weight function has around $\pm k_p$ a small weight, so the program does not optimize the steep slope(which is not of interest) of this part of the operator. Comparing these results with the previous results we see that in the wavenumber band of interest the optimized operators are significantly better. The spatial operators have also a better decaying character for larger offsets.

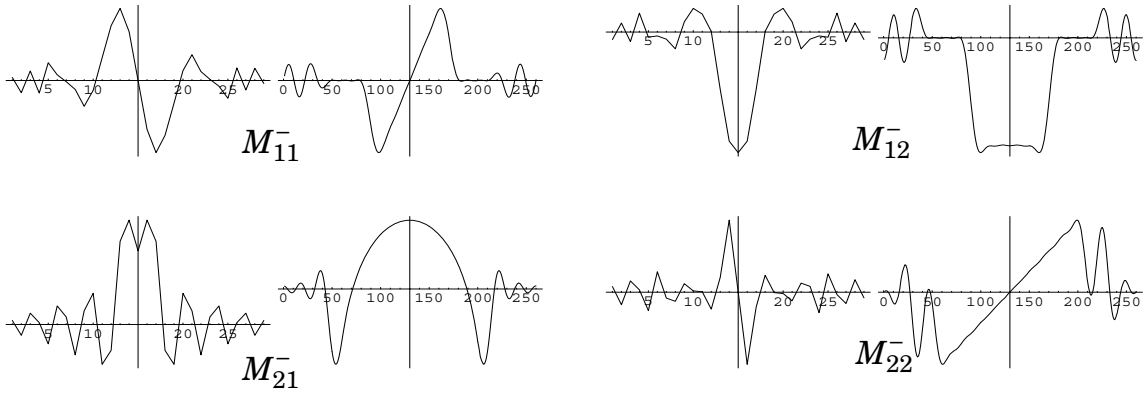

Fig. D.7 *Spatial decomposition operators calculated with a specific weight function. Left is the spatial operator, right the real part of the wavenumber spectrum of this operator.*

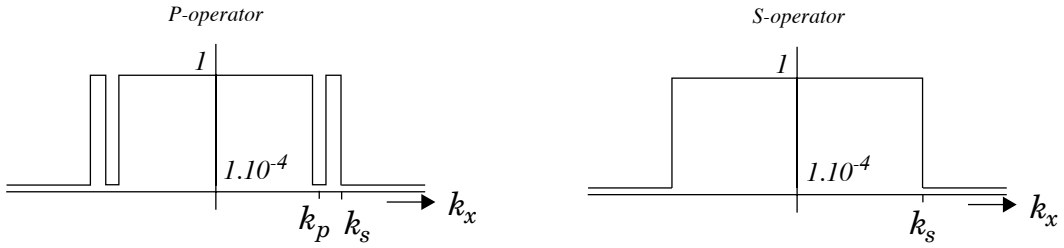

Fig. D.8 *Specific weight functions for the P and S decomposition operators.*

D.4 Decomposition with optimized short spatial operators

To compare the different computational methods for the decomposition process a simple reference model was chosen in a convenient way such that the particle velocity measurements contain the response of one distinct P- and S-wave. This reference model is shown in Figure D.9; a pressure source is placed just below an interface 600 meters below the free-surface, the receivers are placed at the free-surface. By placing the source just below an interface conversion into P and S-waves takes immediately place after the wave has traveled through the interface.The receiver decomposition at the free surface should decompose the field completely in

P and S-waves. The particle velocity (measured in x- and z-direction) recordings of the model are computed by using a staggered finite difference program which interpolates the V_x position to the V_z position.

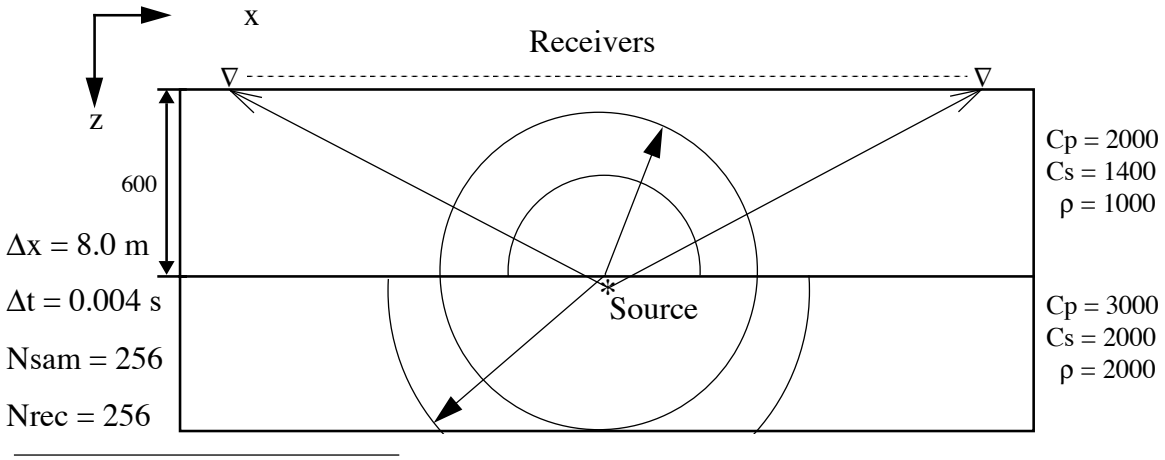

Fig. D.9 *The model used in the finite difference program to calculate the particle velocity records. The source is placed just below the interface and the receivers are placed at the Free-surface.*

A snapshot of this model is shown in Figure D.10. In this snapshot we can see three different head waves. The head wave between the lower P wave and the upper S-wave can also be observed in the particle velocity measurements.

Fig. D.10 *Snapshot after 0.4 seconds, note the two head waves.*

The V_x and V_z measurements are shown in Figure D.11. From these pictures the distinct P and S waves can be seen and the S head wave, on the slope of the S-wave hyperbola, is also present, the P-head wave is not observed. At the bottom of these pictures some boundary effects of the finite difference program are present and a P-wave multiple.

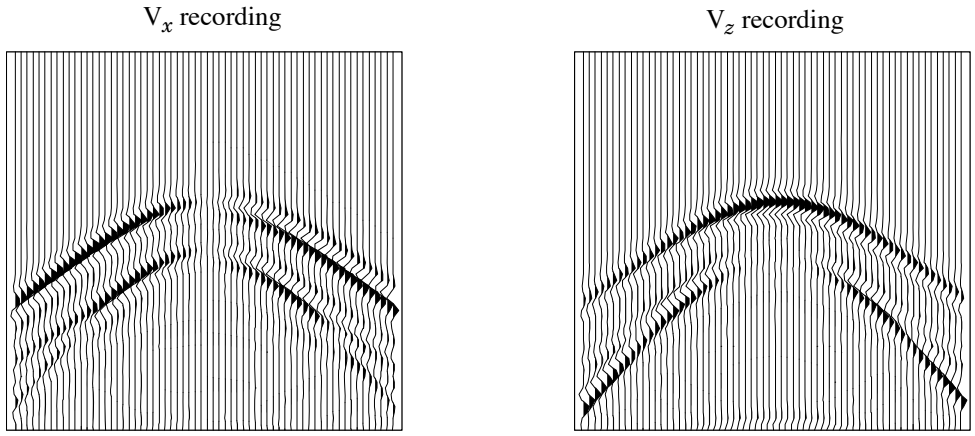

Fig. D.11 *Particle velocity recordings of the synthetic model shown in Figure D.9.*

The result of decomposition by multiplication in the wavenumber-frequency domain is shown in Figure D.12. Note that this process is only allowed if the surface layer is laterally homogeneous along the receiver array, so laterally inhomogeneous layers cannot be taken into account. The advantage of calculation in this domain is that the decomposition operators are exactly known and that the computation is fast. However, a disadvantage is that computation in the wavenumber-frequency domain may lead to strong boundary effects and artifacts due to the finite length of the receiver array and the limited recording time (see Figure D.12). To reduce the influence of the edge effects zero's can be padded to the input data to make the edges further away from the significant data, but then the computation time of the 2-Dimensional Fourier transform becomes less attractive. Another way to reduce the edge effects is to taper the edges in the space-time domain, but then information in the data is distorted.

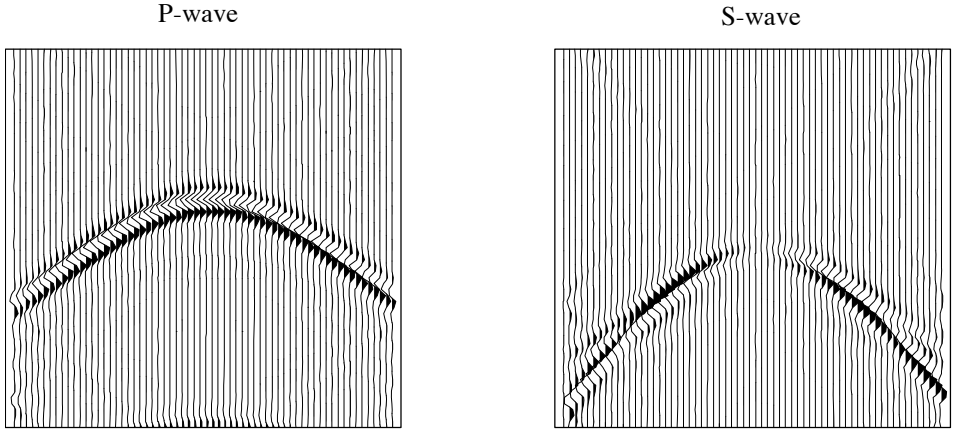

Fig. D.12 *Decomposition of the synthetic model by multiplication in the wavenumber-frequency domain.*

In Figure D.12 the decomposition result is shown where a spatial operator is used. The spatial operator is obtained by truncating the Fourier transformed results to 29 points (which is identical with a unit weight function).

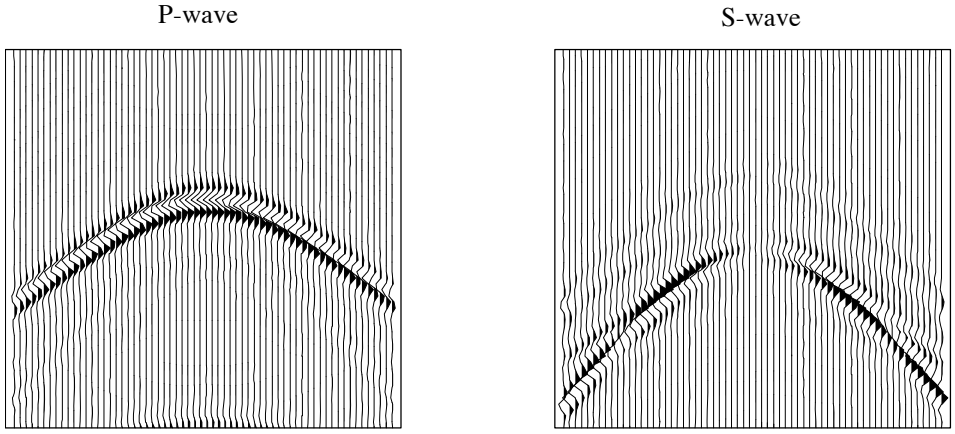

Fig. D.13 *Decomposition of the synthetic model using truncated spatial operators which were calculated by taking a unit weight function (**I**).*

Using the optimized spatial decomposition operators gives the results shown in Figure D.12.

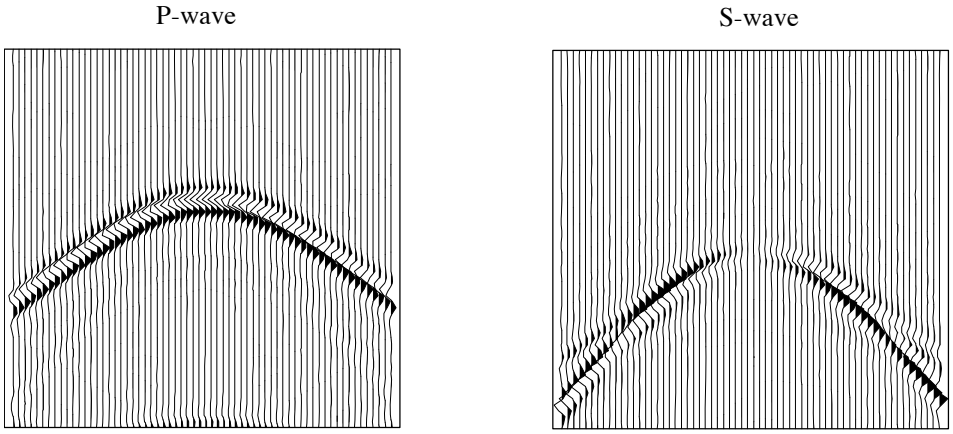

Fig. D.14 *Decomposition of the synthetic model in space-frequency domain using optimized operators.*

In conclusion we can say that the optimized decomposition operators give the best decomposition results. A disadvantage of this procedure is that the calculation time for these operators is

relatively long compared with the wavenumber decomposition. In the near future we will look at shorter operators by optimizing the weight function.

References

Abramowitz, M. and Stegun, I.A., 1965, *Handbook of mathematical functions*, New York, Dover Publishing Co.

Berkhout, A.J., 1984, *Seismic resolution; resolving power of acoustical echo techniques*, Handbook of geophysical exploration; Volume 12, Geophysical Press.

Claerbout, J.F., 1985, *Fundamentals of geophysical data processing*, Blackwell Cs. Publishers.

Herrmann, P.C., 1992, *Decomposition of multi-component measurements into P and S waves*, PHD thesis, Delft University of Technology.

Wapenaar, C.P.A., and Berkhout, A.J., 1989, *Elastic wave field extrapolation, Redatuming of single-and multi-component seismic data*, Elsevier Science Publishers.